

# AMORE-HX: a multidimensional optimization of radial enhanced NMR-sampled hydrogen exchange

John M. Gledhill Jr. · Benjamin T. Walters ·  
A. Joshua Wand

Received: 10 June 2009 / Accepted: 29 June 2009 / Published online: 26 July 2009  
© Springer Science+Business Media B.V. 2009

**Abstract** The Cartesian sampled three-dimensional HNCO experiment is inherently limited in time resolution and sensitivity for the real time measurement of protein hydrogen exchange. This is largely overcome by use of the radial HNCO experiment that employs the use of optimized sampling angles. The significant practical limitation presented by use of three-dimensional data is the large data storage and processing requirements necessary and is largely overcome by taking advantage of the inherent capabilities of the 2D-FT to process selective frequency space without artifact or limitation. Decomposition of angle spectra into positive and negative ridge components provides increased resolution and allows statistical averaging of intensity and therefore increased precision. Strategies for averaging ridge cross sections within and between angle spectra are developed to allow further statistical approaches for increasing the precision of measured hydrogen occupancy. Intensity artifacts potentially introduced by over-pulsing are effectively eliminated by use of the BEST approach.

**Keywords** Hydrogen exchange · Radial sampling · Angle selection · Two-dimensional FT

## Introduction

Hydrogen exchange phenomena remain a rich source of information about protein folding, stability, dynamics and function (Englander and Kallenbach 1983; Krishna et al. 2004). Because the dominant native (hydrogen bonded) state of the protein is hydrogen exchange inactive, hydrogen exchange methods are often able to detect fractional populations of non-native states on the order of  $10^{-10}$  with ease and precision. This unparalleled access to the free energy manifold of proteins allows insights that are difficult or impossible to achieve by other experimental approaches. Hydrogen exchange methodology has evolved greatly over the past few decades. Tritium-based monitoring of exchange (Englander 1963) to near single amide site resolution by peptide fragmentation (Englander et al. 1985) has been generally supplanted by two-dimensional  $^1\text{H}$ - $^1\text{H}$  and  $^1\text{H}$ - $^{15}\text{N}$  correlation spectroscopy [e.g. (Fuentes and Wand 1998a; Wagner and Wüthrich 1982; Wand et al. 1986)]. These methods have allowed comprehensive studies of protein hydrogen exchange phenomena under a range of physical perturbations such as temperature [e.g. (Milne et al. 1999)], denaturant [e.g. (Bai et al. 1995)] and pressure [e.g. (Fuentes and Wand 1998b)]. More recently, hydrogen exchange monitored by mass spectrometry and peptide fragmentation has emerged to be a practical tool for studies of larger proteins that are problematic for two-dimensional NMR methods (Englander 2006).

The resolution provided by two-dimensional sampling often becomes limiting for hydrogen-exchange studies of proteins larger than 300 amino acids. Three-dimensional sampling of hydrogen exchange via the standard HNCO experiment decreases the time resolution by an order of magnitude and often renders this approach inappropriate. Various methods have been introduced to decrease the

---

John M. Gledhill and Benjamin T. Walters have contributed equally to this work.

---

J. M. Gledhill Jr. · B. T. Walters · A. J. Wand (✉)  
Department of Biochemistry & Biophysics, University  
of Pennsylvania, 905 Stellar-Chance Laboratories, 422 Curie  
Blvd., Philadelphia, PA 19104-6059, USA  
e-mail: wand@mail.med.upenn.edu

acquisition time of such multidimensional experiments. One approach focuses on optimization of the longitudinal relaxation properties (Lescop et al. 2007; Schanda and Brutscher 2005; Schanda et al. 2005; Schanda et al. 2006). In addition, sparse sampling techniques such as radial sampling (Coggins and Zhou 2008; Kupce and Freeman 2005) with its attendant processing schemes (Coggins and Zhou 2006; Kazimierczuk et al. 2006; Kupce and Freeman 2004; Marion 2006; Yoon et al. 2006; Gledhill and Wand 2007) can also be used to achieve significant time-savings.

Here we adapt the radial sampling technology to the collection of real time hydrogen exchange data. Various unique features of the radial sampling strategy are exploited to increase the time resolution, sensitivity and accuracy of large protein hydrogen exchange data collection using the HNC0. For a three-dimensional NMR experiment, radial sampling is achieved by linking the two indirect dimensions and linearly sampling a vector at an angle ( $\alpha$ ) with respect to the two orthogonal time domains (Kupce and Freeman 2004). This is achieved by collecting the directly detected time domain signal normally and linking the indirect dimensions by defining  $t_1 = \tau \cos(\alpha)$  and  $t_2 = \tau \sin(\alpha)$  and linearly sampling the time period  $\tau$  (Kupce and Freeman 2004). Such data can be processed to three dimensional frequency space using a back-projection approach (Kupce and Freeman 2004) or a true two dimensional Fourier transformation (Coggins and Zhou 2006; Kazimierczuk et al. 2006; Marion 2006). The latter offers a number of advantages that we will employ here. In the context of protein hydrogen exchange rates determined in real time, the primary task is the proper determination of peak intensity as a function of exchange time. Therefore, optimal angle selection becomes essential in order to provide resolution of peak intensity in at least one component angle spectrum. We have previously described a simple geometric method to determine if peak intensity is resolved at a given angle of radially sampled incremented time domains (Gledhill and Wand 2008). We now describe an algorithm to optimize angle selection with regard to peak resolution and redundancy across multiple sampling angles when the chemical shifts are known. Maltose binding protein (MBP), a 41 kD ABC transporter from *E. coli* is used as a model system.

## Materials and methods

The MBP gene was subcloned from *E. coli* genomic DNA into a pGEM vector and then subcloned using NdeI and BamHI restriction sites into the pET11a vector expression vector. A methionine at position 1 and an I3T mutation were inserted during cloning. This protein sequence is identical to that reported by Gardner et al. (Gardner et al.

1998). The protein was purified as described (Chun et al. 1993). The NMR sample used was 1 mM  $^{15}\text{N}^{13}\text{C}$ -MBP prepared in 20 mM potassium phosphate, 2 mM  $\beta$ -cyclodextrin, 3  $\mu\text{M}$   $\text{NaN}_3$ , 100  $\mu\text{M}$  EDTA at pH\* 7.6. NMR data were obtained at 310 K on a 500 MHz ( $^1\text{H}$ ) Bruker Avance III NMR spectrometer equipped with a triple resonance cryoprobe. Data were processed with an in-house computer program that will be described elsewhere.

## Results

Fourier transformation of radially sampled time domain data results in a fundamental artifact manifested as a ridge of intensity extending through the peak positions at  $\pm 90^\circ$  the radial sampling angle. A number of algorithms have been introduced to remove these ridges (Kupce and Freeman 2004; Venters et al. 2005; Yoon et al. 2006) though such processing is shown to be unnecessary in the context of measuring hydrogen exchange (see below). Briefly, the approach resolves individual radial angle spectra using traditional FFT of the directly detected  $^1\text{H}$  dimension. The component radial spectra of the resulting interferogram are generated using a direct two-dimensional Fourier transform (2D-FT). This is illustrated in Fig. 1. If two authentic peaks fall on the same ridge vector, the ridge intensity is the sum of the two peak intensities (notice three ridges in Fig. 1g whereas in Fig. 1e two of the three peaks are coincident). The ridges can be separated into the positive (Fig. 1g, h) and negative (Fig. 1e, f) angle components by using a sum and difference of matching and non-matching Fourier transforms (Gledhill and Wand 2007).

We have termed the general approach to be described here a multidimensional optimization for radially enhanced NMR-based hydrogen exchange in proteins or AMORE-HX. The strategy is to optimize radial angle selection in the context of an array of novel processing and statistical strategies for the collection of hydrogen exchange information in large proteins. Recently we have described a best-first sorting algorithm to identify a minimal set of radial sampling angles that resolve all or a defined set of cross peaks (Gledhill and Wand 2008).

Individual HNC0 angle experiments are collected sequentially rather than interleaved to allow for increased resolution of exchange time points. The amount of data resulting from sampling HX using three-dimensional spectra is substantial. The directly detected dimension is transformed with a standard FFT to produce an interferogram while non-standard methods are introduced for processing the indirect radial sampled dimensions. Typically the linked dimensions of radial sampled data are processed with a direct 2D-FT for the entire frequency range defined by the sampling increment. However, this is too time

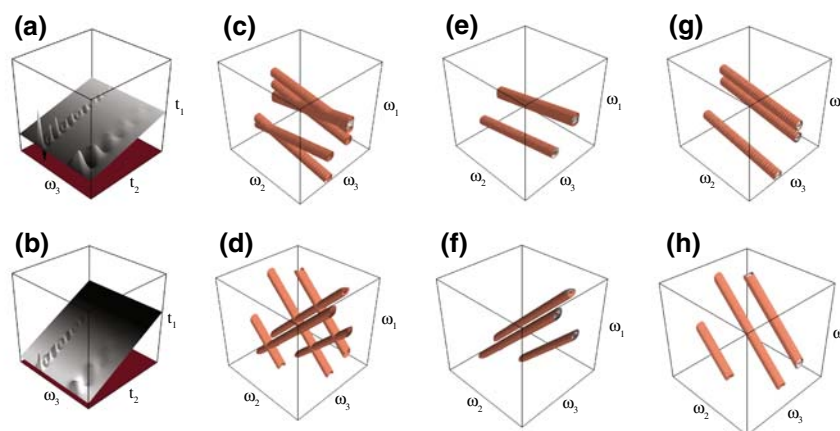


**Fig. 1** Schematic illustration of the decomposition of radial sampled spectra. The radial interferograms from a fictitious spectrum containing three peaks, after FFT of the direct  $^1\text{H}$  dimension (F3), is shown for  $10^\circ$  (a) and  $45^\circ$  (b). The simultaneous 2D-FT of radial sampled data results in ridge artifacts that are shown as *cylinders* in

3D frequency space. The ability to separate positive and negative components (Gledhill and Wand 2007) is a distinct advantage of the discrete FT. The positive (e, f) and negative components (g, h) are shown after separation for angles  $10^\circ$  and  $45^\circ$ , respectively

consuming and data storage intensive and is unnecessary. Two alternate methods, termed sub-window and orthogonal vector processing, are employed.

In contrast to the FFT, the direct 2D-FT can process a limited frequency range without artifact. From the initial chemical shift list, the locations of authentic cross peaks and corresponding artifact ridges can be directly defined and a limited frequency range (sub-window) processed with the 2D-FT (Fig. 2). This circumvents having to process every indirect plane in its entirety; only those regions containing maximum intensities need be processed for visual inspection, if desired. Vectors orthogonal to resolved ridge intensity are extracted using the 2D-FT.

Using the standard equations for a ridge (Gledhill and Wand 2008), each intensity on the orthogonal vector is determined directly using the 2D-FT by supplying the corresponding paired frequency components. As the 2D-FT is rigorously a linear transform the resulting one-dimensional vector is a linear measure of the hydrogen occupancy. This also allows averaging of the orthogonal vectors from various angle components. The vector length is chosen to be sufficient to allow for fitting of peak lineshape. This approach provides an enormous saving in processing time.

A final consideration is the potential sensitivity of hydrogen exchange in large proteins sampled by NMR

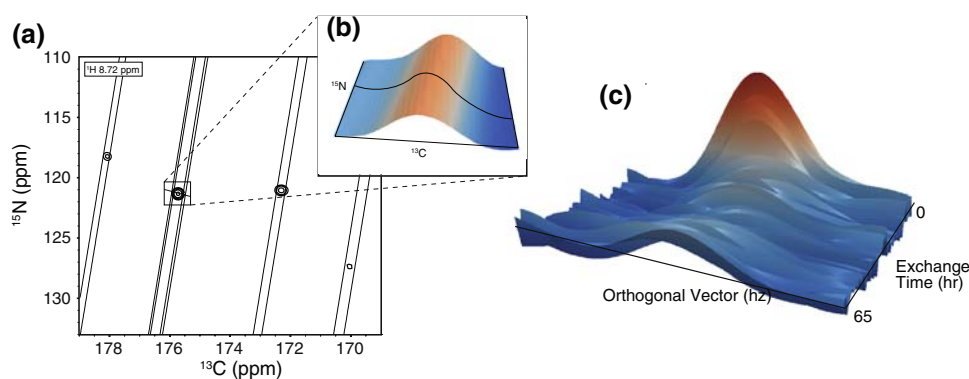


**Fig. 2** The vector orthogonal to the ridge arising from each resolved peak is obtained directly from the 2D-FT. If desired, a two-dimensional sub-window can also be generated by the use of the 2D-FT. The ability to extract one and two-dimensional subspaces is a fundamental property of the 2D-FT and is achieved by simply defining the desired frequency space. a An example of the sub-window and orthogonal vector selection is demonstrated by overlaying the Cartesian sampled spectrum upon the  $10^\circ$  positive sloped

ridge component spectrum from the hydrogen exchange data set (see Fig. 4). b Using the 2D-FT, frequency pairs are transformed as dictated by points along the *orthogonal vector*, which are easily obtained by simple trigonometry (Gledhill and Wand 2008). c *Stacked plot* of orthogonal vectors for residue A360 obtained at different hydrogen exchange time points are shown for each of the sequential  $+10^\circ$  spectra. Obtained at 500 MHz ( $^1\text{H}$ )

spectroscopy to the effects on the relaxation properties of an amide hydrogen by substitution of neighboring amide sites with deuterium. This will be manifested in both longitudinal and transverse relaxation. The latter influences maximum peak intensity and can be avoided by employing cross peak integrals (volumes). The former influences peak intensity through non-equilibrium effects introduced by over-pulsing. A small but not insignificant effect is seen in the maltose binding protein. To assess this, the apparent  $^1\text{H}$   $T_1$  was measured by inversion recovery sampled using the  $^{15}\text{N}$ -HSQC. Though only an approximation,  $^1\text{H}$  recovery curves were fitted to a single exponential. Effective  $^1\text{H}$   $T_1$ s of amide hydrogens in the protein prepared in 90%  $\text{H}_2\text{O}$ :10%  $\text{D}_2\text{O}$  buffer are compared to that obtained in 50%  $\text{H}_2\text{O}$ :50%  $\text{D}_2\text{O}$  buffer (Fig. 3). The difference averages  $7 \pm 6\%$  indicating a small but not insignificant effect that would introduce a second order error in amide hydrogen intensities over the course of an exchange experiment under conditions of incomplete relaxation of amide  $^1\text{H}$  spins during the recycle delay. Here the advantages of the BEST approach (Lescop et al. 2007; Schanda and Brutscher 2005; Schanda et al. 2005; Schanda et al. 2006) are particularly useful. For  $^{13}\text{C}$ ,  $^{15}\text{N}$ -MBP, the apparent amide  $^1\text{H}$   $T_1$ s, measured using the conventional HNC0, of protein prepared in 90%  $\text{H}_2\text{O}$  buffer had a mean deviation from protein prepared in 50%  $\text{H}_2\text{O}$  of  $-35 \pm 40\%$ . In contrast, the apparent amide  $^1\text{H}$   $T_1$ s, measured using the BEST HNC0, of protein prepared in 90%  $\text{H}_2\text{O}$  buffer had a mean fractional deviation from protein prepared in 50%  $\text{H}_2\text{O}$  of  $+0.06 \pm 0.24$ . Delays as short as 0.1 s could be used without introduction of this relaxation artifact.

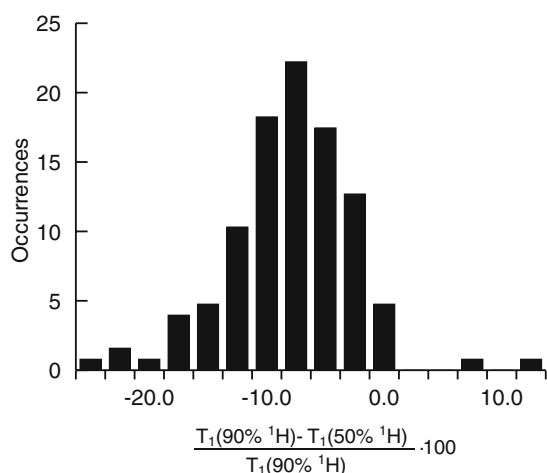


**Fig. 3** Effect of increasing deuterium occupancy on amide  $^1\text{H}$  longitudinal relaxation in maltose binding protein. Apparent amide  $^1\text{H}$   $T_1$  values were estimated by inversion recovery sampled with  $^{15}\text{N}$ -HSQC spectra of MBP prepared in 90%  $\text{H}_2\text{O}$ :10%  $\text{D}_2\text{O}$  buffer and 50%  $\text{H}_2\text{O}$ :50%  $\text{D}_2\text{O}$  buffer. Obtained at 500 MHz ( $^1\text{H}$ )

Following dissolution into deuterium buffer, hydrogen exchange of maltose binding protein (370 amino acids; 349 non-proline residues) was monitored in real-time by sequential acquisition of radially sampled components of a sensitivity-enhanced radially sampled BEST HNC0. Exchange rates for maltose binding protein were determined at 500 MHz at 310 K and  $\text{pH}^* 7.6$ . A peak list was determined from a Cartesian sampled HNC0 experiment and was filtered (Gledhill and Wand 2008) for (near) degenerate peaks that would never be resolved by radial sampling employing a small set of sampling angles. The overlapping peaks were replaced with single peaks that had a combined line width of both peaks. The angle selection resulted in four angles ( $69^\circ$ ,  $81^\circ$ ,  $10^\circ$ ,  $27^\circ$ ) that resolved 307 of the 334 cross peaks resolved in the conventional Cartesian HNC0 spectrum obtained at 500 MHz ( $^1\text{H}$ ). Only 203 cross peaks are resolved in the corresponding  $^{15}\text{N}$ -HSQC spectrum. Inclusion of an additional angle would resolve only one more peak, making inclusion of additional angles inefficient. The angle data sets were collected sequentially using a 0.6 s recycle delay over a 65 h period resulting in 70 angle sets for 280 total experiments. All free induction decays were processed with the FFT. Using the starting peak list as a reference, all perpendicular vectors for the positive and negative angle ridge components for each peak were automatically processed using the 2D-FT. These vectors are generated for all of the angles collected. Gaussian lineshapes are fitted to each vector and maximum intensities or integrals are extracted for each time point.

Visualization of the exchange data as a stacked-plot of orthogonal vectors with respect to time is shown for residue D197 of MBP in Fig. 4. Exchange rate information from 2D HX experiments such as the  $^{15}\text{N}$ -HSQC is usually obtained by fitting the time dependent change in signal volume or maximal intensity to a single exponential decay. It is important to emphasize that individual component spectra are employed here. The fully processed three-dimensional spectrum is unnecessary. Only those individual orthogonal vectors, from individual positive and negative components, having resolved peak intensity for a given cross peak are used to obtain hydrogen occupancy. Resolution is determined algorithmically (Gledhill and Wand 2008).

The precision of the obtained rate of hydrogen exchange can be increased by appealing to the multiple measurements contained within each angle data set. Each radial sampling angle produces two component spectra with uncorrelated noise. The redundancy can be exploited in multiple ways such as averaging the intensity data from each angle component vectors or averaging rates fitted from each component. Two caveats to this approach relate to the time-resolution needed. Fast exchanging peaks

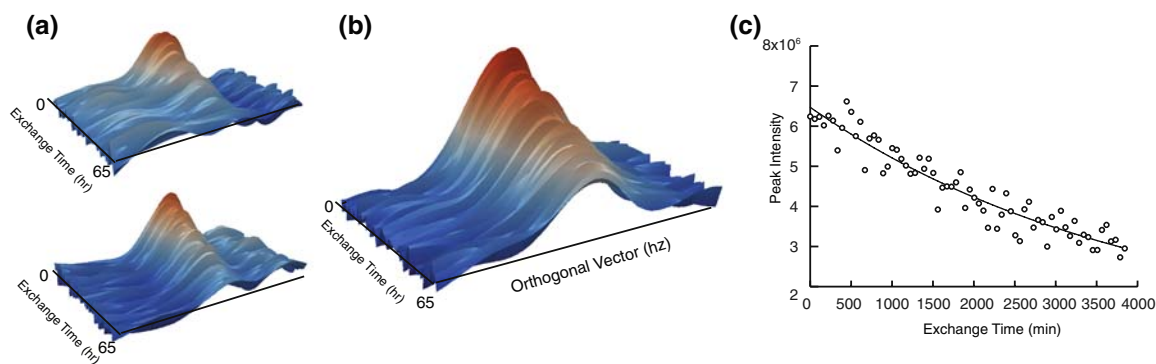


**Fig. 4** AMORE-HX sampled hydrogen exchange in maltose binding protein. Shown are data for residue D197. **a** Two of the 8 component spectra ( $\pm 69^\circ$ ) are shown as *stacked plots*. **b** The *S/N* is increased by averaging all 8 component spectra. **c** The one dimensional slice of the

averaged stacked plot at maximum intensity is then fitted with a single exponential to obtain an exchange rate of  $(2.5 \pm 0.8) \times 10^{-4} \text{ min}^{-1}$ . Obtained at 500 MHz ( $^1\text{H}$ )

require greater time-resolution whereas slower exchanging residues can be resolved with equivalent accuracy over longer intervals. An example of averaging the orthogonal vectors for each of the resolved angles is shown in Fig. 4. For fast exchanging peaks, orthogonal vectors are not averaged which decreases the time-resolution to the experimental time required for collecting an individual angle. In this case, the rates are determined by taking each resolved angle sequentially as the next time-point. Conversely, for slowly exchanging amides, resolved by multiple angles, the orthogonal vectors for each resolved angle component per angle set can be averaged. In that case the time resolution becomes the sum of the acquisition times for all of the angles averaged. However, because noise is uncorrelated between components of a single angle or between angles, averaging increases the precision of the obtained hydrogen exchange rate (Fig. 4). In these ways, sampling and processing strategies can be balanced to achieve optimum *S/N* throughout the course of exchange. The obtained hydrogen exchange rates generally agree with rates independently measured conventionally with  $^{15}\text{N}$ -HSQC spectra to better than 25%, which is essentially the usual precision of hydrogen exchange rates measured by standard real-time NMR using the  $^{15}\text{N}$ -HSQC. As the dynamic range of amide HX in proteins is often  $10^{10}$  this level of precision is more than satisfactory.

We have illustrated the basic ideas of the AMORE-HX method using an angle set defined by the “best first” approach outlined previously (Gledhill and Wand 2008). It turns out that the best-first sorting algorithm can result in a suboptimal set of angles because resolved peak identity is not considered when selecting an angle. This can result in the selection of more angles than are necessary. For most applications, where the entire three-dimensional space is

examined, this is generally not a significant hindrance. However, as is clear above, the most compact set of sampling angles is desirable for the collection of hydrogen exchange data i.e. one that will select a set of angles based on the uniqueness of the angle, paying particular attention to peaks that are resolved by relatively few angles. This can be achieved by using a system of weights designed to circumvent the time required for a combinatorial approach. The first step is to determine which peaks are resolved over the set of all angles. The resolution data is tabulated in a  $M \times N$  Boolean matrix,  $A$ , where  $N$  is the total number of cross peaks and  $M$  is total number of angles to choose from. For a given peak and angle combination,  $a_{nm}$ , is set to true if the peak is resolved by the given angle and false if it is not resolved. A peak is determined to be resolved using the ridge-to-ridge distance algorithm described previously (Gledhill and Wand 2008).

To generate a measure of resolution for each peak we define a count matrix  $C$  as the dot product of a unity row matrix of length  $M$  and the Boolean resolution data matrix  $A$ .

$$C = [1, k, 1_M] \times A. \quad (1)$$

The vector  $C$  contains an inventory of the number of times a peak is resolved for each radial sampling angle. We define a weight function to facilitate choosing angles based on uniqueness:

$$\omega(C) = 1 - \frac{C}{\max(C)}. \quad (2)$$

$\max(C)$  is the largest element of  $C$ . The elements of the weight function  $\omega(C)$  approaches unity when a peak is only resolved by a small number of angles. This allows a direct measure of which peaks are hard to resolve and the ability to determine which angles resolve these peaks. The

next angle to be selected corresponds to the maximum value of the measures function generated from the dot product between the Boolean matrix  $A$  and the transposed weight function  $\omega(C)$

$$\mu(C^T) = A \times \omega(C)^T. \quad (3)$$

Each element in the measures function,  $\mu(C^T)$ , corresponds to the sum of the now weighted terms in  $A$ . The angle identified by  $\max(\mu(C))$  is selected. Subsequent angles are selected after  $A$  is modified to remove all peaks resolved by the selected angle and the process repeated until the desired number of peaks are resolved. Selecting angles that resolve the more rarely resolved peaks is often more efficient than selecting the angles that resolve the most peaks first. Angle selection is essential to AMORE-HX as appropriate selection of sampling angles will ensure minimal acquisition time per decay time points. Applying this angle selection to the HNCO spectrum of MBP at 500 MHz ( $^1\text{H}$ ) results in a set of three angles (25, 15, 44) that resolved 309 of the 334 cross peaks that are resolvable. This decreases the minimum sampling time by 25%.

## Discussion

The use of conventional Cartesian sampled three-dimensional HNCO spectra for real time measurement of protein hydrogen exchange is inherently limited in time resolution. This is largely overcome by use of the radial HNCO experiment that employs use of an optimized set of sampling angles. A refined angle selection routine has been developed to aid in the process of angle selection. Two significant practical limitations of measuring hydrogen exchange using three-dimensional experiments are the large data storage and processing time requirements necessary. This can be largely overcome by taking advantage of the inherent capability of the two-dimensional FT to process selective frequency space without artifact or limitation. In addition, the ability to decompose the individual angle spectra into so-called positive and negative ridge components not only potentially provides increased resolution but also opens the possibility for statistical averaging of intensity and therefore increased precision. Using the 42 kDa MBP as an illustrative example, sufficient  $S/N$  and digital resolution was obtained at 500 MHz to allow  $\sim 15$  min time resolution for real time measurement of hydrogen exchange even using a relatively long recycle interval. The time resolution could be much shorter (approximately 3 min) if the full advantage of the BEST modification of the HNCO was utilized and the recycle delay reduced to the minimum allowable 0.1 s. It is further noted that even more complex angle sets could be

employed to increase the time resolution at early stages of the acquisition for desired cross peaks. This flexibility is inherent to the radial sampling strategy but prohibited by standard Cartesian sampling. Finally, strategies for averaging ridge cross sections within and between angle spectra have been presented that allow further statistical approaches to increasing the precision of measured hydrogen occupancy. One would anticipate that monitoring large protein hydrogen exchange in real-time at very modest magnetic fields will be enabled by use of the various tools presented here.

**Acknowledgments** Supported by the Mathers Foundation, NIH grant DK 39806 and an NSF MRSEC award (DMR-0520020). J.M.G. is supported by NIH predoctoral training grant GM 008275. We thank Alison Wand and Dr. Sabrina Bédard for construction of the MBP expression vector and Shoshanna Pokras for helpful discussion.

## References

- Bai YW, Sosnick TR, Mayne L, Englander SW (1995) Protein-folding intermediates—native state hydrogen exchange. *Science* 269:192–197
- Chun SY, Strobel S, Bassford P Jr, Randall LL (1993) Folding of maltose-binding protein. Evidence for the identity of the rate-determining step in vivo and in vitro. *J Biol Chem* 268:20855–20862
- Coggins BE, Zhou P (2006) Polar Fourier transforms of radially sampled NMR data. *J Magn Reson* 182:84–95
- Coggins BE, Zhou P (2008) High resolution 4-D spectroscopy with sparse concentric shell sampling and FFT-CLEAN. *Journal of Biomolecular NMR* 42:225–239
- Englander SW (1963) A hydrogen exchange method using tritium and sephadex its application to ribnuclease. *Biochemistry* 2:798–807
- Englander SW (2006) Hydrogen exchange and mass spectrometry: a historical perspective. *J Am Soc Mass Spec* 17:1481–1489
- Englander SW, Kallenbach NR (1983) Hydrogen-exchange and structural dynamics of proteins and nucleic acids. *Quarterly Reviews of Biophysics* 16:521–655
- Englander JJ, Rogero JR, Englander SW (1985) Protein hydrogen-exchange studied by the fragment separation method. *Analytical Biochemistry* 147:234–244
- Fuentes EJ, Wand AJ (1998a) Local dynamics and stability of apocytochrome b(562) examined by hydrogen exchange. *Biochemistry* 37:3687–3698
- Fuentes EJ, Wand AJ (1998b) Local stability and dynamics of apocytochrome b(562) examined by the dependence of hydrogen exchange on hydrostatic pressure. *Biochemistry* 37:9877–9883
- Gardner KH, Zhang XC, Gehring K, Kay LE (1998) Solution NMR studies of a 42 kDa Escherichia coli maltose binding protein beta-cyclodextrin complex: chemical shift assignments and analysis. *J Am Chem Soc* 120:11738–11748
- Gledhill JM, Wand AJ (2007) Phasing arbitrarily sampled multidimensional NMR data. *J Magn Reson* 187:363–370
- Gledhill JM Jr, Wand AJ (2008) Optimized angle selection for radial sampled NMR experiments. *J Magn Reson* 195:169–178
- Kazimierzuk K, Kozminski W, Zhukov I (2006) Two-dimensional Fourier transform of arbitrarily sampled NMR data sets. *J Magn Reson* 179:323–328
- Krishna MM, Hoang L, Lin Y, Englander SW (2004) Hydrogen exchange methods to study protein folding. *Methods* 34:51–64

- Kupce E, Freeman R (2004) Projection-reconstruction technique for speeding up multidimensional NMR spectroscopy. *J Am Chem Soc* 126:6429–6440
- Kupce E, Freeman R (2005) Fast multidimensional NMR: radial sampling of evolution space. *J Magn Reson* 173:317–321
- Lescop E, Schanda P, Brutscher B (2007) A set of BEST triple-resonance experiments for time-optimized protein resonance assignment. *J Magn Reson* 187:163–169
- Marion D (2006) Processing of ND NMR spectra sampled in polar coordinates: a simple Fourier transform instead of a reconstruction. *J Biomol NMR* 36:45–54
- Milne JS, Xu YJ, Mayne LC, Englander SW (1999) Experimental study of the protein folding landscape: unfolding reactions in cytochrome c. *Journal of Molecular Biology* 290:811–822
- Schanda P, Brutscher B (2005) Very fast two-dimensional NMR spectroscopy for real-time investigation of dynamic events in proteins on the time scale of seconds. *J Am Chem Soc* 127:8014–8015
- Schanda P, Kupce E, Brutscher B (2005) SOFAST-HMQC experiments for recording two-dimensional heteronuclear correlation spectra of proteins within a few seconds. *J Biomol NMR* 33:199–211
- Schanda P, Van Melckebeke H, Brutscher B (2006) Speeding up three-dimensional protein NMR experiments to a few minutes. *J Am Chem Soc* 128:9042–9043
- Venters RA, Coggins BE, Kojetin D, Cavanagh J, Zhou P (2005) (4, 2)D projection-reconstruction experiments for protein backbone assignment: application to human carbonic anhydrase II and calbindin D-28K. *J Am Chem Soc* 127:8785–8795
- Wagner G, Wüthrich K (1982) Amide proton exchange and surface conformation of the basic pancreatic trypsin inhibitor in solution: studies with two-dimensional nuclear magnetic resonance. *Journal of Molecular Biology* 160:343–361
- Wand AJ, Roder H, Englander SW (1986) Two dimensional <sup>1</sup>H NMR studies of cytochrome c—hydrogen exchange in the N-terminal helix. *Biochemistry* 25:1107–1114
- Yoon JW, Godsill S, Kupce E, Freeman R (2006) Deterministic and statistical methods for reconstructing multidimensional NMR spectra. *Magn Reson Chem* 44:197–209